the film refractive index was calculated by using the Lorentz–Lorenz equation which assumes an average of water and polymer refractive indices. Hence, our picture of the polymer monolayer is that of an extremely hydrated one. Microscopic models which take into account individual molecular polarizability[10,13,14,26] predict that $\delta\Delta$ is linear with θ. Unfortunately, within experimental error we cannot discern between linear dependence and that obtained by calculating the average refractive index with the Lorentz–Lorenz equation for the polymers studied here. Further experiments with other monolayers of higher ellipsometric contrast are in progress to address this issue.

Acknowledgment. This work is in part supported by the Research Committee of the University of Wisconsin—Madison and the Procter and Gamble Company.

Registry No. PEO, 25322-68-3; HPC, 9004-64-2; PVAc, 9003-20-7; PMMA, 9011-14-7.

References and Notes

(1) Smith, T. *J. Opt. Soc. Am.* **1968**, *58*, 1069.
(2) de Feijter, J. A.; Benjamins, J.; Veer, F. A. *Biopolymers* **1978**, *17*, 1759.
(3) Graham, D. E.; Phillips, M. C. *J. Colloid Interface Sci.* **1979**, *70*, 415.
(4) Kawaguchi, M.; Oohira, M.; Tajima, M.; Takahashi, A. *Polym. J. (Tokyo)* **1980**, *12*, 849.
(5) de Feijter, J. A.; Benjamins, J. *J. colloid Interface Sci.* **1981**, *81*, 91.
(6) den Engelsen, D.; de Koning, B. *J. Chem. Soc., Faraday Trans. 1* **1974**, *70*, 1603.
(7) den Engelsen, D.; de Koning, B. *J. Chem. Soc., Faraday Trans. 1* **1974**, *70*, 2100.
(8) Kawaguchi, M.; Yohyama, M.; Mutoh, Y.; Takahashi, A. *Langmuir* **1988**, *4*, 407.
(9) Kawaguchi, M.; Yohyama, M.; Takahashi, A. *Langmuir* **1988**, *4*, 411.
(10) Rasing, Th.; Hsiung, H.; Shen, Y. R.; Kim, M. W. *Phys. Rev. A* **1988**, *37*, 2732.
(11) Kim, M. W.; Sauer, B. B.; Yu, H.; Yazdanian, M.; Zografi, G., to be submitted for publication.
(12) Archer, R. *J. Opt. Soc. Am.* **1962**, *52*, 970.
(13) Archer, R. J. In *Ellipsometry in the Measurement of Surfaces and Thin films*; Passaglia, E., Stromberg, R. R., Kruger, J., Eds.; NBS Miscellaneous Publication 256; U.S. Government Printing Office: Washington, DC, 1964; p 255.
(14) Bootsma, G. A.; Meyer, F. *Surf. Sci.* **1969**, *14*, 52.
(15) Crisp, D. J. *J. Colloid Sci.* **1946**, *1*, 49.
(16) Crisp, D. J. *J. Colloid Sci.* **1946**, *1*, 161.
(17) Vilanove, R.; Rondelez, F. *Phys. Rev. Lett.* **1980**, *45*, 1502.
(18) Kawaguchi, M.; Komatsu, S.; Matsuzumi, M.; Takahashi, A. *J. Colloid Interface Sci.* **1984**, *102*, 356.
(19) Kawaguchi, M.; Sano, M.; Chen, Y.-L.; Zografi, G.; Yu, H. *Macromolecules* **1986**, *19*, 2606.
(20) Kuzmenka, D. J.; Granick, S. *Polym. Commun.* **1988**, *29*, 64.
(21) Ries, H. E.; Walker, D. C. *J. Colloid Sci.* **1961**, *16*, 361.
(22) Gabrielli, G.; Guarini, G. G. T. *J. Colloid Interface Sci.* **1978**, *64*, 185.
(23) Azzam, R. M. A.; Bashara, N. M. *Ellipsometry and Polarized Light*; North Holland: New York, 1977.
(24) Huglin, M. B., Ed. In *Light Scattering From Polymer Solutions*; Academic: New York, 1972; p 35.
(25) *Polymer Handbook*; Brandrup, J., Immergut, E. H., Eds.; Wiley: New York, 1975.
(26) Strachan, C. S. *Proc. Cambridge Philos. Soc.* **1933**, *29*, 116.
(27) Hall, A. C. *J. Phys. Chem.* **1966**, *70*, 1702.
(28) Sauer, B. B.; Yu, H.; Kim, M. W. *Langmuir*, in press.
(29) *Handbook of Water-Soluble Gums and Resins*; Davidson, R. L., Ed.; McGraw-Hill: New York, 1980.
(30) Rastogi, A. K.; St. Pierre, L. E. *J. Colloid Interface Sci.* **1971**, *35*, 16.

Chain Dimensions in Dilute Polymer Solutions: A Light-Scattering and Viscometric Study of Multiarmed Polyisoprene Stars in Good and Θ Solvents

Barry J. Bauer,[1a] Lewis J. Fetters,*[1b] William W. Graessley,[1c] Nikos Hadjichristidis,[1d] and Günther F. Quack[1e]

Institute of Polymer Science, University of Akron, Akron, Ohio 44325, and Corporate Research Laboratories, Exxon Research and Engineering Company, Annandale, New Jersey 08801. *Received August 31, 1988; Revised Manuscript Received November 23, 1988*

ABSTRACT: The dilute solution properties of long-arm polyisoprene stars with branch point functionality f ranging from 3 to 56 have been investigated both in good solvents (cyclohexane and toluene) and under Θ conditions (1,4-dioxane). The intrinsic viscosity $[\eta]$, Huggins coefficient k_H, second virial coefficient A_2, diffusion coefficient D_0, and radius of gyration R_G were measured and compared in terms of the equivalent radii. A smooth evolution of properties with increasing f was found, leading eventually to what we have termed a fuzzy-sphere behavior at high f. Thus, equilibrium properties such as A_2 and R_G move into a spherelike relationship to one another at large f. The dynamical properties, $[\eta]$ and D_0, do likewise, and k_H approaches the hard-sphere value. However, the radii deduced from dynamical properties are consistently smaller than those from equilibrium properties, suggesting the analogy between polymeric stars of larger functionality and spheres with a hydrodynamically penetrable surface layer. The dependence of size on functionality is different in good and Θ solvents, but the same fuzzy-sphere relationship emerges when f is large. The literature data for polystyrene stars follow the same pattern, being for the most part in quantitative accord with the polyisoprene data. Some unresolved descrepancies in this simple interpretation are pointed out. Good agreement was found between these results and theoretical predictions based on scaling, Monte Carlo calculations, and simulation. Analytical expressions were less satisfactory, especially at high functionality.

Introduction

A study of the dilute solution properties of linear polyisoprene in the thermodynamically good solvent cyclohexane was presented recently.[2] Dilute solution viscometry and light scattering were used to obtain the radius of gyration R_G, the thermodynamic radius R_T, the viscometric radius R_V, and the hydrodynamic radius R_H. The molecular weight dependence of these various measures of coil dimensions was determined. The results were compared with theory and with data for other polymer species. In

0024-9297/89/2222-2337$01.50/0

Table I
Molecular Structure and Dilute Solution Properties of Three- and Four-Arm Star Polyisoprenes in Cyclohexane

sample[a]	$M \times 10^{-4}$, g mol^{-1}	$M_a \times 10^{-4}$, g mol^{-1}	$\bar{f}$	$A_2 \times 10^4$, mL mol g^{-2}	$[\eta]$, dL g^{-1}	k_H
3-II	3.52	1.14	3.1	12.6	0.354	0.33
4-II	4.65	1.14	4.1	12.4	0.376	0.35
3-I	5.06	1.70	3.0	11.6	0.450	0.33
4-I	6.80	1.70	4.0	10.4	0.480	0.36
3-VI	11.1	3.67	3.0	9.0	0.803	0.42
4-VI	14.8	3.67	4.0	8.9	0.869	0.37
3-III	13.7	4.40	3.1	8.7	0.958	0.36
4-III	17.3	4.40	3.9	8.5	0.973	0.34
3-VIII	13.9	4.75	2.9	8.4	0.979	0.40
4-VIII	18.8	4.75	4.0	8.1	1.03	0.41
3-V	21.1	7.22	2.9	7.7	1.34	0.38
4-V	28.0	7.22	3.9	8.0	1.45	0.39
3-IV	27.8	9.50	2.9	7.1	1.65	0.36
4-IV	38.0	9.50	4.0	7.3	1.74	0.37
3-VII	32.2	10.5	3.1	7.0	1.85	0.40
4-VII	41.0	10.5	3.9	7.0	1.95	0.46

[a] The paired three- and four-arm star samples were prepared by organochlorosilane linking by using the same batch of polyisoprenyllithium precursor: each pair has the same arm molecular weight, M_a.

the present paper we extend the study to multiarm polyisoprene stars and include data obtained under Θ conditions as well. The main issue to be considered here is the dependence of coil dimensions on branch point functionality, with particular emphasis on the long-arm limit. Samples with constant chain microstructure, narrow molecular weight distribution, and up to 56 arms per molecule were prepared by anionic polymerization methods. Molecular weight M, second virial coefficient A_2, and radius of gyration were determined by light scattering; intrinsic viscosity $[\eta]$ and Huggins coefficient k_H were determined viscometrically. The diffusion coefficient at infinite dilution, D_0, was also obtained for selected samples. The data were organized in terms of equivalent radii and compared with the behavior of spheres and the predictions of molecular theory.

Experimental Section

The synthesis procedures used to prepare the polyisoprene stars have been described elsewhere.[3-5] The initiators were purified *sec*-butyl- or *tert*-butyllithium (Lithium Corp. of America); the linking agents were multifunctional chlorosilanes[3,4] and divinylbenzene.[5] The polymerization conditions used led to a statistically uniform stereoirregular chain microstructure (~7% 3,4; ~70% cis-1,4; ~23% trans-1,4).[3,4,6,7] The chlorosilane linking agents were used to prepare a series of 3-, 4-, 5-, 8-, 12-, and 18-arm polyisoprene stars; in some cases, a small amount of butadiene was added just prior to linking to facilitate that reaction. Within each of these series the arm molecular weight was varied while the number of branches per molecule was kept constant. Four additional series of stars were prepared by divinylbenzene linking. Within each of these series the number of branches per molecule was varied while the arm molecular weight was kept constant. In all cases a small aliquot of arm was withdrawn prior to linking for subsequent determination of the branch point functionality.

Light-scattering measurements were made with a Sofica PGD photometer (wide-angle light scattering (WALS)), a Chromatix KMX-6 photometer (low-angle laser light scattering (LALLS)), and a Brookhaven photometer and correlator (quasi-elastic light scattering (QELS)). Methods of solvent purification are described elsewhere.[3,4,6] Measurements were made for a series of concentrations well below the overlap concentration $c^* \sim [\eta]^{-1}$. The WALS and the LALLS data were used to determine the weight-average molecular weight $M_w = M$, the z-average radius of gyration $\langle R_G^2 \rangle_z^{1/2} = R_G$, and the second virial coefficient A_2 by procedures described in the earlier paper.[2] The QELS data were used to determine the diffusion coefficient at infinite dilution, D_0, and the concentration coefficient k_D:

$$D(c) = D_0(1 + k_D c + ...) \quad (1)$$

Flow times for solvent and several polymer concentrations below c^* were measured in Cannon-Ubbelohde capillary viscometers and used to determine the intrinsic viscosity $[\eta]$ and the Huggins coefficient k_H:

$$\frac{\eta - \eta_s}{\eta_s c} = [\eta](1 + k_H[\eta]c + ...) \quad (2)$$

Data were obtained in good solvents and under Θ conditions. For the good solvent case, the light-scattering results were obtained in cyclohexane at 23 °C, and the viscometric results were obtained in cyclohexane at 25 °C and toluene at 34 °C (Tables I–IV). The difference between these two solvents appears to be negligible, at least judged by viscometric data. Thus, within experimental error, and as noted recently by others,[6] the same Mark–Houwink–Sakurata equation describes $[\eta]$ vs M for linear polyisoprene in both cyclohexane[2,6] and toluene:[7]

$$[\eta] = 1.65 \times 10^{-4} M^{0.745} \quad (\text{dL g}^{-1}) \quad (3)$$

We also determined $[\eta]$ in both toluene and cyclohexane for several of the branched samples (Tables II and IV) and found no systematic differences. More detailed comparisons are summarized in the Appendix. We will treat these solvents as being "equivalently good" in the subsequent discussions.

The Θ solvent used was 1,4-dioxane. A Flory temperature θ of 34 ± 1 °C had been obtained earlier[7] for linear polyisoprenes of this microstructure by measuring A_2 (light scattering) at several temperatures and interpolating to the temperature at which $A_2 = 0$. Hadjichristidis and Roovers found θ to be unchanged for four- and six-arm polyisoprene stars.[7] However, we have found that θ is reduced in the more highly branched stars, evaluated elsewhere[8] and in this study (Tables II and III). The change appears to become negligible, however, for sufficiently long arms, as shown in Figure 1. Similar results have been found for multiarm polystyrene stars.[9-13] Although the effects of branching on the Θ temperature seem quite regular, we were unable to rationalize the systematics in terms of the existing theory.[8,14] Also, neither arm molecular weight, M_a, nor total molecular weight, M, provides a unified correlation of θ (Figure 1a and 1b). We assume that the composite character of segment density for highly branched stars, a crowded core and more dilute exterior as opposed to the uniformly low segmental density of linear chains, is somehow responsible. In the absence of clear alternatives, the values of $(R_G)_\theta$, $[\eta]_\theta$, and $(k_H)_\theta$ reported in Tables II and III were measured at θ as determined for each sample by the $A_2 = 0$ condition. We assume that any effects associated with θ variations are small, especially so for our work here, which emphasizes behavior for large M_a.

All stars were fractionated to remove unattached arms.[3,4] The average number of arms per molecule for the resulting samples (Tables I and II) was calculated from the arm molecular weight M_a and the total molecular weight M as obtained by light scattering or, in a few cases, by osmotic pressure:

$$\bar{f} = M/M_a \quad (4)$$

Table II
Molecular Characteristics of Chlorosilane-Linked Polyisoprene Stars

			Θ condition				good solvent			
sample	$M \times 10^{-4}$, g mol^{-1}	$\bar{f}$[a]	θ, °C	R_G, nm	$[\eta]$, dL g^{-1}	k_H	R_G, nm	$[\eta]$,[b] dL g^{-1}	k_H[b]	$A_2 \times 10^4$, mL mol g^{-2}
5-I	15.0	5.0	33.2		0.365	0.71		0.77	0.35	7.5
5-II	25.0	4.9	33.0		0.454	0.68		1.03	0.40	6.5
8-VIII	4.1	8.0	29.8		0.140	0.66		0.250[d]	0.46	7.4
8-VII	11.0	7.9	31.0		0.232	0.63		0.420	0.52	6.8
8-I	27.6	7.4	32.9		0.364	0.69		0.875	0.52	5.9
8-II	61.0	6.9	32.7		0.555	1.0	25.5	1.50	0.44	4.9
8-III	79.5	8.1	32.7	19.5	0.625	0.92	30.1	1.84	0.55	4.5
8-VI	171	8.1	33.2	28.3[c]	0.895	1.0	44.1	3.20	0.52	3.2
8-IV	176	7.8	33.2	29.0	0.900	1.5	45.5	3.25	0.56	3.1
8-V	440	8.3	32.6	45.0	1.43	1.6	75.1	6.20	0.61	2.2
8-IX	600	7.9	33.5	52.4[c]	1.64	3.0	90.0	7.80	0.53	2.0
12-IX	4.1	11.7	21.0		0.110	0.77		0.225[d]	0.53	9.4
12-IV	9.6	11.6	25.8		0.170	0.60	7.3[e]	0.280	0.72	5.5
12-VII	25.0	11.9	28.7		0.269	0.65		0.580	0.80	4.5
12-I	41.2	11.6	32.6		0.352	0.78		0.800	0.74	3.9
12-II	81.0	11.8	32.0	17.8	0.484	0.90	25.0	1.36	0.57	3.4
12-III	144	12.0	32.9	24.2	0.665	0.95	35.2	2.14	0.79	3.0
12-VIII	390	12.0	33.0	39.4[c]	1.09	1.2	58.7	4.23	0.69	1.9
12-V	528	12.2	33.0	44.4[c]	1.24	2.4	72.0	5.55	0.68	1.9
18-VII	6.4	17.9	24.5		0.094	1.0	4.9[e]	0.144[d]	0.63	6.4
18-VIII	9.3	18.0	26.8		0.112	0.92		0.180	0.88	6.0
18-VI	19.7	18.0	28.1		0.178	1.1		0.351	0.75	4.4
18-II	21.8	18.0	29.0		0.190	1.2	9.6[e]	0.371	0.67	3.9
18-I	38.4	18.1	30.0		0.238	1.3		0.529	0.63	3.2
18-III	80.0	17.4	31.0		0.356	1.4	21.4	1.02	0.78	2.7
18-IV	148	18.0	32.0	22.0	0.470	3.3	29.9	1.62	0.71	2.3
18-V	357	17.9	33.0	33.3	0.708	5.2	50.0	2.92	0.71	2.0
18-IX	680	17.4	33.2	45.5	1.01	9.2	70.0	5.07	0.88	1.6

[a] Average star functionality: values of M_a from either light scattering or osmometry reported in prior publications; ref 3, 4, and 8. [b] Measured in toluene. [c] Obtained with Fica 50 photometer (ref 8). [d] Values not used in calculations due to departures from linear chain power law behavior when $2M_a$ is $\leq 10^4$. [e] Obtained by neutron scattering in benzene-d_6 (ref 15).

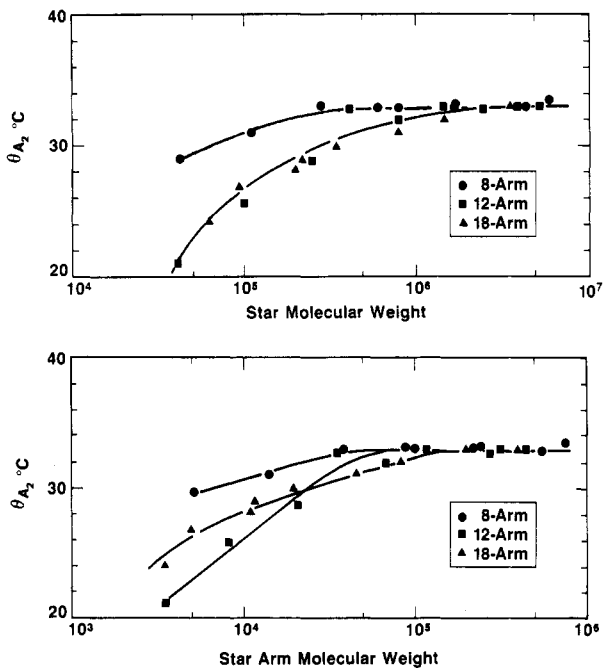

Figure 1. (a, Top) Θ temperature as a function of polyisoprene star molecular weight. (b, Bottom) Θ temperature as a function of polyisoprene star arm molecular weight.

The close agreement between $\bar{f}$ and the functionality of the chlorosilane linking agent used in each case is gratifying and indicates a highly uniform molecular structure for those stars. No direct comparison of this kind is available for the divinylbenzene-linked stars, and some distribution in functionality is of course inevitable. However, the linking statistics should be no more heterodisperse than those for a Poisson distribution, so at large $\bar{f}$ the distribution is probably rather narrow.[5] Size exclusion chromatograms for the divinylbenzene-linked stars were

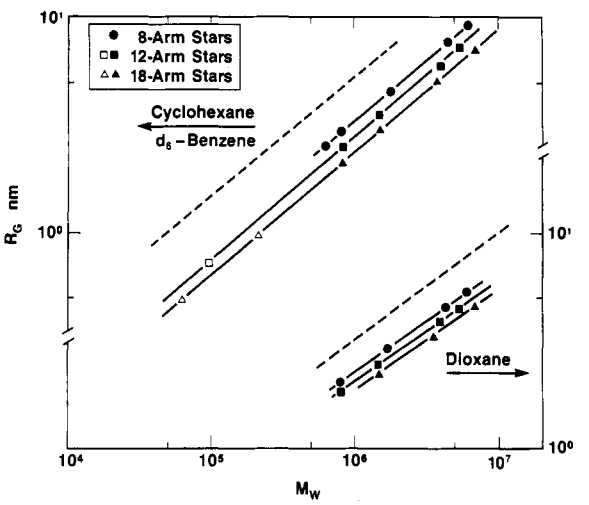

Figure 2. Neutron-scattering (open symbols) and light-scattering (solid symbols) based radii of gyration of polyisoprene stars. The dashed lines denote linear polyisoprene.

only marginally broader, if at all, than those for the stars prepared by chlorosilane linking. Differences in polydispersity, especially in the high molecular weight tail, could present a problem in dealing with R_G because it is a z-average quantity. However, as noted below, we have found no significant difference between chlorosilane-linked and divinylbenzene-linked samples in the correlations.

Analysis of Results

The chlorosilane-linked stars provide information on arm length effects at constant branching architecture. Radius of gyration as a function of total molecular weight for the 8-, 12-, and 18-arm architectures in both good and Θ solvents is compared with the corresponding data for linear polyisoprene in Figure 2. (The light-scattering-

Table III
Molecular Characteristics of Divinylbenzene-Linked Polyisoprene Stars

				Θ condition				good solvent			
sample	$M_a \times 10^{-4}$, g mol^{-1}	$M \times 10^{-4}$, g mol^{-1}	$\bar{f}$[a]	θ, °C	R_G, nm	$[\eta]$, dL g^{-1}	k_H	R_G, nm	$[\eta]$,[b] dL g^{-1}	k_H[b]	$A_2 \times 10^4$, mL mol g^{-2}
31	3.9	48.5	12.4	31.0		0.363	0.76	19.0	0.847	0.50	3.6
32		62.5	16.0	30.6		0.346	0.82	19.9	0.835	0.62	2.8
33		64.6	16.6	30.6		0.345	0.82	20.1	0.830	0.69	2.6
34		102.0	26.1	30.6		0.303	0.90	21.4	0.820	0.77	1.9
71	5.1	167.0	32.7	31.2		0.339	1.18	27.0	0.926	0.93	1.5
21	8.4	72.0	8.6	32.2		0.566	0.79	27.7	1.38	0.57	3.2
22		104.0	12.4	32.2		0.504	0.92	29.0	1.37	0.84	3.0
24		188.0	22.4	31.8		0.463	1.19	32.3	1.35	0.98	1.9
11	14.9	155.0	10.2	33.0	26.0	0.705	0.76	39.5	1.90	0.62	3.0
12		178.0	11.9	33.0	27.0	0.650	0.71	41.1	1.95	0.78	2.8
13		340.0	22.2	33.0	31.5	0.625	0.76	47.4	1.90	1.00	1.8
14		840.0	56.2	33.0	37.0	0.525	0.75	54.5	1.85	1.02	0.5

[a] Star polymer functionality: $\bar{f} = M/M_a$, where both M and M_a have been established independently by light scattering or osmotic pressure measurements. [b] Measured in toluene.

Table IV
Hydrodynamic Properties of Selected Polyisoprene Stars in Cyclohexane

sample	$M \times 10^{-4}$, g mol^{-1}	$[\eta]$, dL g^{-1}	k_H	$D_0 \times 10^7$, cm^{-2} s^{-1}	k_D, mL g^{-1}
3-III	13.7	0.958	0.36	2.4	
4-III	17.3	0.973	0.34	1.87	76.5
4-IV	38.0	1.74	0.37	1.20	138
8-III	79.5	1.83	0.60	0.91	235
8-IV	176	3.30	0.71	0.52	250
8-V	440	6.37	0.51		
12-IV	9.6	0.294	0.81		
12-II	81.0			0.89	174
12-VIII	390	4.33	0.58	0.368	560
12-V	528	5.63	0.50	0.305	331
18-VIII	9.3	0.182	0.79		
18-II	21.8			2.4	
18-I	38.4			1.88	35
18-III	80.0	1.02	0.73	1.06	100
18-IV	148	1.58	0.77	0.71	169
18-V	357	2.90	0.78	0.455	303

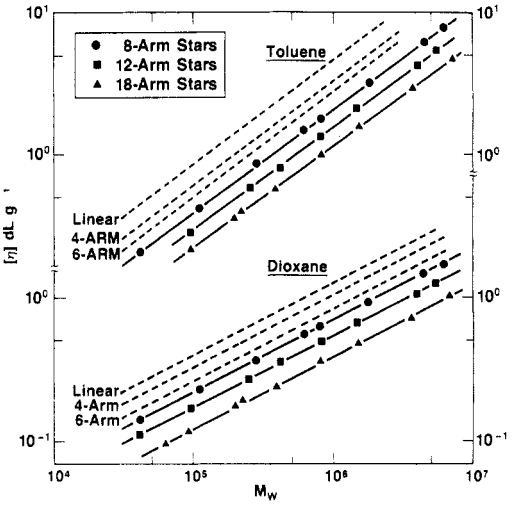

Figure 3. Intrinsic viscosity for polyisoprene stars.

based radii of gyration are supplemented by neutron-scattering results in benzene-d_6 for some short-arm stars.[15]) A sequence of parallel or nearly parallel lines is obtained, showing that the effect of architecture is essentially independent of molecular weight when the branches are long. Similar results have been found in other studies[7,9,10,13] and are expected for sufficiently long arms on the basis of theory.

Figure 3 shows a similar comparison for the intrinsic viscosity. Again the effect of architecture is factorable, in this case demonstrated over a much wider range of molecular weights. Similar behavior is found for the second virial coefficient. The molecular weight dependence of all three properties is well described by power laws:

$$[\eta] = K_V M^{\alpha} \quad (5)$$

$$R_G = K_R M^{\beta} \quad (6)$$

$$A_2 = K_A M^{-\gamma} \quad (7)$$

The main variation with branch architecture is contained in K_V, K_R, and K_A. The values of the coefficients and exponents in eq 5–7, obtained by linear regression of these data and from the literature (see Appendix), are given in Table V. Slight variations in the exponents, mostly the

Table V
Coefficients Describing the Molecular Weight Dependence of Intrinsic Viscosity, Radius of Gyration, and Second Virial Coefficient for Chlorosilane-Linked Polyisoprene Stars[a]

	good solvents						Θ conditions				
structure	$K_V \times 10^4$	α	$K_R \times 10^2$	β	$K_A \times 10^2$	γ	$K_V \times 10^4$	α	$K_R \times 10^2$	β	ref
linear[b]	1.70	0.74_1					12.6	0.05_0	3.27	0.50_0	7, 16
linear[c]	1.93	0.73_5	1.91	0.57_8	1.32	0.23_0					2, 6
3 arm[c]	1.25	0.75_7			1.83	0.26_0					this work
4 arm[b]	1.32	0.73_7					9.1_2	0.50_9	2.69	(0.50)[d]	7
4 arm[c]	1.16	0.75_3			1.54	0.23_8					this work
6 arm[b]	0.98_9	0.74_3					8.4_8	0.49_8	2.27	(0.50)[d]	7
8 arm[b]	0.94_7	0.72_6	1.78	0.54_6	1.89[c]	0.28_5	7.5_5	0.49_3	2.56	0.48_9	this work
12 arm[b]	0.57_0	0.74_1	1.37	0.55_5	2.27[c]	0.31_0	5.3_9	0.50_1	2.31	0.49_0	this work
18 arm[b]	0.30_4	0.76_4	1.09	0.55_8	0.66[c]	0.24_0	3.7_4	0.50_2	2.53	0.47_6	this work

[a] See eq 5–7. Units are dL g^{-1} for $[\eta]$, nm for R_G, and mL mol g^{-2} for A_2. [b] Measurement made in toluene. [c] Measurement made in cyclohexane. [d] Theoretical exponent used in order to establish K_R from limited data (three samples for four- and six-arm star polyisoprene samples, respectively).

Table VI
Size Parameters (nm) in Cyclohexane for Chlorosilane-Linked Three- and Four-Arm Polyisoprene Stars

sample	R_V	R_T	sample	R_V	R_T
3-II	5.8	5.4	4-II	6.5	6.4
3-I	7.1	6.7	4-I	8.0	7.8
3-VI	11.2	10.3	4-VI	12.7	12.5
3-III[a]	12.8	11.7	4-III[b]	13.9	13.6
3-VIII	12.9	11.7	4-VIII	14.5	14.2
3-V	16.5	15.0	4-V	18.6	18.4
3-IV	19.4	17.6	4-IV[c]	21.9	21.9
3-VII	21.1	19.8	4-VII	23.3	22.7

[a] R_H = 9.6 nm. [b] R_H = 12.3 nm. [c] R_H = 19.2 nm.

result of experimental scatter and limited data, make it difficult to draw quantitative conclusions directly from the K_V, K_R, and K_A values in the table.

Another way of examining the results is to convert the values of $[\eta]$, A_2, and D_0 into equivalent radii based on the respective equations for hard spheres:[2,17,18]

$$R_V = 5.41 \times 10^{-9}([\eta]M)^{1/3} \quad (8)$$

$$R_T = 4.63 \times 10^{-9}(A_2M^2)^{1/3} \quad (9)$$

$$R_H = 5.31 \times 10^{-2}kT/\eta_s D_0 \quad (10)$$

where η_s is the solvent viscosity, k is Boltzmann's constant, R_V is the viscometric radius, R_T is the thermodynamic (excluded volume) radius, and R_H is the hydrodynamic radius. For monodisperse spheres, $R_V = R_T = R_H = (5/3)^{1/2}R_G$. Dilute solution theories for the effects of branching on R_G, A_2, D_0, and $[\eta]$ are traditionally written[19] in terms of parameters such as g, h, g', the Flory coefficients P and ϕ, and the penetration function ψ (see below). We have chosen to express the results in a slightly different way here. For example, in place of ψ we use R_T/R_G, and in place of g we use $R_G/(R_G)_a$, where $(R_G)_a$ is the radius of gyration of an unattached arm. Both ψ and g contain precisely the same information as R_T/R_G and $R_G/(R_G)_a$, but the choice is not a completely arbitrary one. Thus, as seen below, the variation of R_T/R_G with f displays in an explicit fashion the growing resemblance of star molecules to spheres as the functionality increases, and the variation of $R_G/(R_G)_a$ with f demonstrates directly the

Table VII
Size Parameters (nm) for Chlorosilane-Linked Polyisoprene Stars with 5, 8, 12, and 18 Arms

	good solvents				Θ conditions	
sample	R_G	R_H	R_V[a]	R_T	R_G	R_V
5-I			12.2	11.9		9.5
5-II			16.0	15.9		12.2
8-VIII			5.1	5.0		4.5
8-VII			9.0	9.3		7.4
8-I			15.6	16.5		11.7
8-II	25.5	25.4	24.3	26.3		17.5
8-III	30.1		28.5 (28.5)	30.4	19.5	19.9
8-VI	44.1		44.2	45.3	28.3	28.9
8-IV	45.5	44.4	44.9 (45.1)	45.6	29.0	29.3
8-V	75.1		75.5 (76.3)	75.0	45.0	46.4
8-IX	90.0		90.5	89.4	52.4	53.8
12-IX			5.3	5.4		4.1
12-IV	7.3		7.5 (7.6)	7.9		6.4
12-VII			13.2	14.1		10.2
12-I			17.3	18.7		13.2
12-II	25.0	25.9	25.9	28.1	17.8	18.4
12-III	35.2		36.5	39.5	24.2	24.7
12-VIII	58.7	62.7	63.9 (64.4)	65.9	39.4	40.7
12-V	72.0	75.0	77.4 (77.7)	80.7	44.4	47.0
18-VII	4.9		5.5	6.5		4.6
18-VIII			6.4 (6.5)	8.0		5.5
18-VI			10.3	11.9		8.2
18-II	9.6	9.5	10.9	12.3		8.7
18-I		12.3	14.8	16.7		11.3
18-III	21.4	21.8	23.3 (23.5)	25.8		16.5
18-IV	29.9	32.5	33.6 (33.3)	36.8	22.0	22.2
18-V	50.0	50.8	54.9 (54.7)	63.2	33.3	34.2
18-IX	70.0		81.7	90.1	45.5	47.7

[a] Based on $[\eta]$ in toluene. The values in parentheses were obtained from $[\eta]$ in cyclohexane.

Table VIII
Size Parameters (nm) for Divinylbenzene-Linked Polyisoprene Stars

		good solvents			Θ conditions	
sample	$\bar{f}$	R_G	R_V	R_T	R_G	R_V
31	12.4	19.0	18.7	20.3		14.1
32	16.0	19.9	20.2	22.1		15.1
33	16.6	20.1	20.4	21.9		15.2
34	26.1	21.4	23.7	27.0		17.0
71	32.7	27.0	29.0	34.6		20.8
21	8.6	27.7	25.0	25.4		18.6
22	12.4	29.0	28.2	31.6		20.2
24	22.4	32.3	34.2	40.5		24.0
11	10.2	39.5	36.0	41.4	26.0	25.8
12	11.9	41.1	38.0	44.5	27.0	26.3
13	22.2	47.4	46.7	59.1	31.5	32.3
14	56.2	54.5	62.7	70.5	37.0	41.2

Table IX
Radius Ratio and Huggins Coefficients for Polyisoprene Stars in Good Solvents

$\bar{f}$	R_T/R_G	R_T/R_V[a]	k_H[b]
linear	0.69	0.87	0.27 (0.34)[c]
3		0.92	(0.37)[c]
4		(0.99)[d]	0.34 (0.38)[c]
5		0.99	0.38
6		(1.02)[d]	0.37
8	1.01	1.02	0.52
12	1.24	1.05	0.69
18	1.27	1.14	0.74
12.4	1.06	1.09	0.50
16.0	1.11	1.10	0.62
16.6	1.09	1.07	0.69
26.1	1.27	1.14	0.77
32.7	1.28	1.19	0.93
8.6	0.92	1.02	0.57
12.4	1.09	1.12	0.84
22.4	1.25	1.18	0.98
10.2	1.05	1.15	0.62
11.9	1.09	1.17	0.78
22.2	1.25	1.25	1.00
56.2	1.30	1.12	1.02

[a] Values of R_V obtained from $[\eta]$ in toluene; other values obtained from cyclohexane data unless otherwise noted. [b] Measured in toluene unless otherwise noted. [c] Measured in cyclohexane. [d] Values of R_T obtained from A_2 in toluene (osmotic pressure).

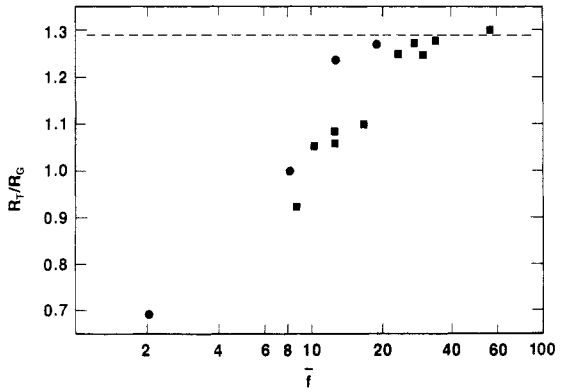

Figure 4. Ratio of thermodynamic radius to radius of gyration as a function of arm number for polyisoprene stars. The chlorosilane-linked stars are denoted by ● and the divinylbenzene-linked stars by ■. The dashed line indicates $R_T/R_G = 1.291$ for hard spheres.

swelling of chain dimensions as the number of arms increases.

Values of R_G, R_T, R_V, and R_H are collected in Tables VI and VII for the chlorosilane-linked stars and in Table VIII for the divinylbenzene-linked stars. The various ratios of radii are then calculated for individual samples; according to the early discussion these ratios should be essentially functions of f alone. The variations with f are examined and compared with the behavior of spheres and finally with the predictions of various molecular theories.

In good solvents the ratios of radii and the values of k_H are practically the same within each series of chlorosilane-linked stars. Their averages, with results for the shortest arm stars omitted in some cases, are given in Table IX. Figure 4 shows the ratio of statically determined radii, R_T/R_G, as a function of branch point functionality in good solvents. Results for both the chlorosilane-linked and divinylbenzene-linked species are included. The values rise rapidly with increasing f from $R_T/R_G = 0.69$ for linear polyisoprene and then level off rather near the hard-sphere value, $R_T/R_G = (5/3)^{1/2} = 1.291$. The approach appears

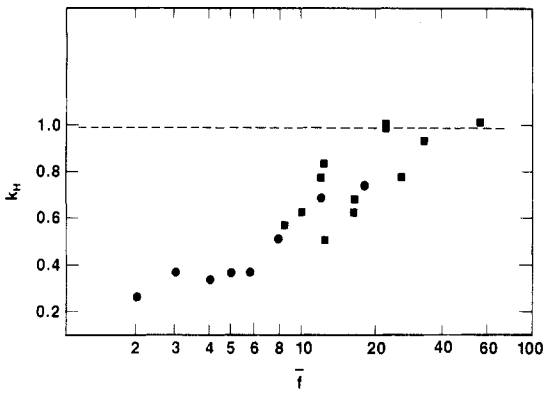

Figure 5. Huggins coefficient as a function of arm number for polyisoprene stars in good solvents. The chlorosilane-linked stars are denoted by ● and the divinylbenzene-linked stars by ■. The dashed line indicates $k_H = 0.99$ for hard spheres.

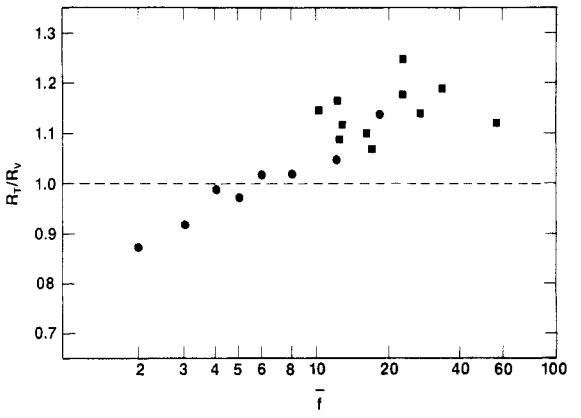

Figure 6. Ratio of thermodynamic radius to viscometric radius as a function of arm number for polyisoprene stars. The chlorosilane-linked stars are denoted by ● and the divinylbenzene-linked stars by ■. The dashed line indicates $R_T/R_V = 1$ for hard spheres.

to be more gradual for the divinylbenzene-linked stars, perhaps because of the slightly broader dispersion of functionalities in those materials, but the limit seems to be the same in both cases.

The ratio of dynamically determined radii, R_V/R_H, is available only for selected samples of the chlorosilane-linked stars (Table VII), and unfortunately those data are somewhat scattered. That ratio is 1.11 for linear polyisoprene,[2] and there appears to be a weak trend toward the hard-sphere value 1.0 at higher f, albeit with considerable scatter. Roovers and Toporowski[17] found R_V/R_H to be near unity for a wide variety of branching architectures in polystyrene.

The dependence of the Huggins coefficient k_H on branch point functionality is shown in Figure 5. The pattern is similar to that found for R_T/R_G and R_V/R_H. The values rise from $k_H = 0.34$ for linear polyisoprene and approach hard-sphere behavior,[20] $k_H = 0.99$, at high functionalities. An unambiguous determination at high f is difficult to achieve, however, because contributions from the higher order terms in eq 2 appear rather quickly when k_H is large.

Comparisons of statically and dynamically determined radii show a similar pattern of dependence on branch point functionality, although the hard-sphere limit at large f seems not to apply in this case. The most plentiful data for comparing static and dynamic radii are those on R_T and R_V; the ratio R_T/R_V is shown as a function of f in Figure 6. The values increase from 0.87 for linear polyisoprene but pass smoothly through the hard-sphere value of unity and appear to scatter around a limit of approximately 1.17,

Table X
Values of R_V/R_G for Polyisoprene Stars in Good Solvents and under θ Conditions

$\bar{f}$	good solvent R_V/R_G	θ conditions R_V/R_G
linear	0.79[a] (0.79)[b]	0.83[c] (0.85)[b]
3	(0.84)[b]	(0.88)[b]
4	(0.91)[b]	0.95 (0.96)[b]
6	(0.99)[b,d]	1.04 (1.07)[b]
8	0.99	1.03
12	1.06 (1.13)[b]	1.04 (1.10)[b]
18	1.11 (1.11)[b,d]	1.03 (1.25)[b,d]
12.4	0.98	
16.0	1.02	
16.6	1.02	
26.1	1.11	
32.7	1.07	
8.6	0.90	
12.4	0.99	
22.4	1.06	
10.2	0.91	0.99
11.9	0.93	0.97
22.2	1.00	1.03
56.2	1.16	1.11

[a] Based on the data of ref 2. [b] Polystyrene results given in parentheses; ref 9, 10, 13, and 17. [c] Based on the data ref 7 and 16. [d] One sample.

the average of values for $f \geq 18$. The analogy to a "fuzzy" sphere,[30b] with deeper hydrodynamic than thermodynamic penetration of the outermost regions occurring even at large f, is suggested.

Thus, it seems that many properties of star polymers in good solvents, including the relationships among static and dynamic measures of chain dimensions, change smoothly from a linear chain limit at low f to some spherelike limit at large f. Such behavior is perhaps not totally unexpected, but it is nevertheless reassuring to find it so clearly evident. It is also useful in providing a framework for the examination of molecular theories.

Results are more limited for branched polyisoprenes at the θ condition. The thermodynamic radius R_T is identically zero, of course, from the $A_2 = 0$ definition, and we have not data on $(R_H)_\theta$ for polyisoprene stars. Furthermore, it is clear from Table II that the values of $(k_H)_\theta$ increase with M_a within each series of chlorosilane-linked stars. Thus, in contrast with k_H in good solvents, $(k_H)_\theta$ is not a function of f alone. The same pattern has also been found for linear polyisoprene[2] and for four- and six-arm polyisoprene stars.[21] Such behavior is contrary to theory[22-26] and also appears to depend somewhat on the polymer species. Thus, for example, $(k_H)_\theta$ in polystyrene systems depends, as expected, only on the branching architecture,[13] but other species show the same anomalies as polyisoprene.[27]

The only radius comparison available for θ conditions is that provided by R_G and R_V. The values of $(R_V/R_G)_\theta$ appear to be independent of M_a within each series of chlorosilane-linked stars. The averages of R_V/R_G under θ conditions and in good solvents are shown in Table X. There is an upward trend with increasing f in both cases, as expected from previous comparisons of radius ratios. However, even at large f the values are smaller than $R_V/R_G = 1.29$ for spheres. As in R_T/R_V for good solvents (Figure 6), we are here comparing a dynamically determined radius with a static one. From the R_T/R_V results and the fuzzy-sphere analogy, we expect a limit of $R_V/R_G = 1.29/1.17 = 1.10$ at large f. The observed values seem to be reasonably consistent with this limit. Interestingly, the values of R_V/R_G for each branching architecture turn out to be about the same in good solvents and θ solvents. We conclude that the "extra" hydrodynamic penetration is roughly similar in good solvents and θ solvents for high functionality stars.

Table XI
Values of $R_V/(R_V)_a$ and $R_G/(R_G)_a$ for Polyisoprene and Polystyrene Stars in Good Solvents and θ Conditions

	good solvents[a]		θ conditions[a]	
$\bar{f}$	$R_V/(R_V)_a$	$R_G/(R_G)_a$	$R_V/(R_V)_a$	$R_G/(R_G)_a$
1	1.00	1.00	1.00	1.00
2	1.50 (1.49)	1.49 (1.50)	1.42 (1.42)	1.41 (1.41)
3	1.78 (1.77)	(1.68)	(1.64)	(1.57)
4	2.01 (2.00)	(1.78)	1.86 (1.83)	1.66 (1.60)
5	2.18		2.01	
6	2.37 (2.33)	(1.91)	2.15 (2.11)	1.68 (1.65)
8	2.57	1.93	2.30	1.88
12	2.93 (2.93)	2.08 (2.10)	2.60 (2.60)	2.10 (2.03)
18	3.33	2.33	2.85	2.28
12.4	2.92	2.16	2.64	
16.0	3.16	2.26	2.82	
16.6	3.19	2.29	2.84	
26.1	3.71	2.43	3.18	
32.7	3.88	2.63	3.40	
8.6	2.48	2.02	2.34	
12.4	2.82	2.12	2.57	
22.4	3.41	2.36	3.05	
10.2	2.58	2.07	2.46	2.06
11.9	2.72	2.15	2.51	2.14
22.2	3.35	2.48	3.09	2.50
56.2	4.50	2.85	3.94	2.93

[a] Values for polystyrene in parentheses: ref 9, 10, 13, and 17.

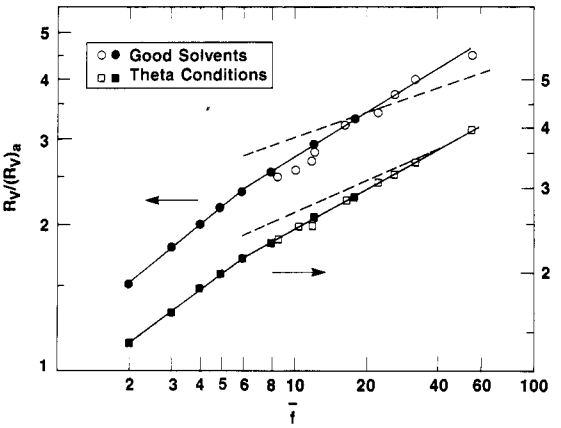

Figure 7. Ratio of viscometric radii for star and unattached arm as a function of arm number for chlorosilane-linked (solid symbols) and divinylbenzene-linked (open symbols) polyisoprene stars. The θ condition three-arm data point is for polystyrene. The dashed lines are predictions based on the fuzzy-sphere picture (see eq 15 and subsequent discussion).

Another comparison of radii can be made by using intrinsic viscosity data alone. The ratio of R_V for a star polymer to $(R_V)_a$, the viscometric radius for the corresponding unattached arm, depends only on f. Values of $(R_V)_a$ were calculated for each star using the known value of M_a and the $[\eta]$ vs M relationships for linear polymers given in Table V. The results are given in Table XI.

The variation of $R_V/(R_V)_a$ with f is shown in Figure 7 for good solvents and at the θ condition. In both cases, the average values of $R_V/(R_V)_a$ for each series of chlorosilane-linked stars and the individual values for divinylbenzene-linked stars lie along the same curve. The relationship between $R_V/(R_V)_a$ and f is, however, somewhat different in good solvents and θ solvents. The generality of the behavior was tested with the published data on chlorosilane- and divinylbenzene-linked polystyrene

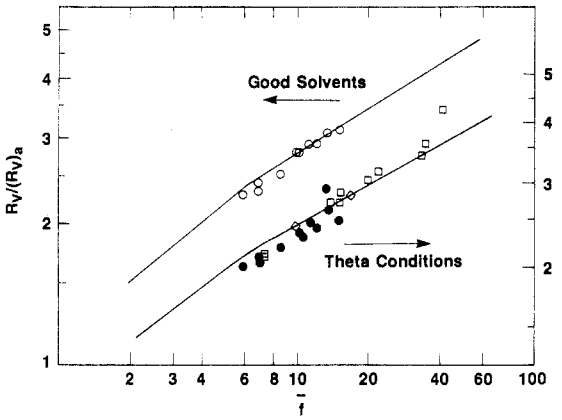

Figure 8. Ratio of viscometric radii for star and unattached arm as a function of arm number for divinylbenzene-linked polystyrene stars: ref 11 (●); ref 28 (□); ref 29 and 30 (◇). The lines are those from Figure 7.

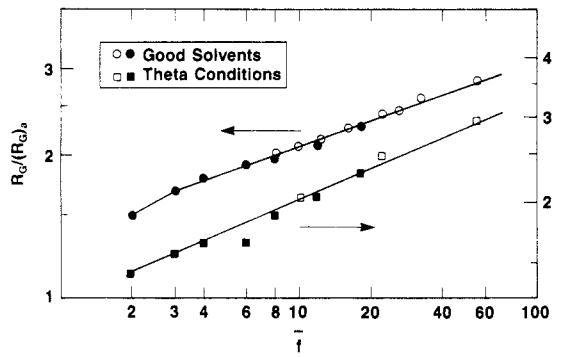

Figure 9. Ratio of radii of gyration for star and unattached arm as a function of arm number for polyisoprene stars. The solid symbols represent the chlorosilane-linked samples, and the open symbols represent the divinylbenzene-linked samples. Polystyrene results are used when the corresponding polyisoprene results are not available (Table XI).

stars.[9-11,13,17,28-30] Comparisons with chlorosilane-linked polystyrene stars are shown in Table XI. The agreement is reasonably good, as shown in Figure 8. As explained elsewhere,[31] we have found such data to be useful for estimating the aggregation number for linear polymers containing a strongly associating group on one end of the chain.

Similar examinations of the reduced radius of gyration, $R_G/(R_G)_a$, were made. Values of $(R_G)_a$ were calculated from M_a by using the results for linear polyisoprene given in the Appendix. Results are shown in Figure 9 for good solvents and at the Θ condition. As in the other comparisons, the average values for chlorosilane-linked stars and the individual values for divinylbenzene-linked stars agree reasonably well. Comparisons with literature data for chlorosilane-linked polystyrene stars[9,10,13,17] are given in Table XI. The value of 12-arm polystyrenes at the Θ condition is slightly smaller, but otherwise the agreement is excellent, so we have included polystyrene values in Figure 9. The literature results for divinylbenzene-linked polystyrene stars[11] do not agree with the polyisoprene data or with the trend of data for chlorosilane-linked polystyrenes. Those values of $R_G/(R_G)_a$ are consistently larger, an observation that we assume is caused by polydispersity.

Aside from the data for six-arm stars at the Θ condition, the results for $f \geq 3$ are described quite precisely by power laws:

$$R_G/(R_G)_a = 1.37f^{0.175} \quad \text{(good solvents)} \qquad (11)$$

$$R_G/(R_G)_a = 1.21f^{0.219} \quad (\Theta \text{ condition}) \qquad (12)$$

Expressions obtained for the chlorosilane-linked stars alone are practically the same ($1.41f^{0.16}$ and $1.22f^{0.21}$, respectively). Even the value of $R_G/(R_G)_a$ for a "two-arm star" under Θ conditions agrees with eq 12. Note that values for individual samples rather than the averages for series were used in the regression analyses here and later to obtain power law exponents and coefficients. Thus, data for each chlorosilane- and divinylbenzene-linked sample were weighted equally. The results obtained by either procedure are practically the same, however.

The behavior for $R_G/(R_G)_a$ and $R_V/(R_V)_a$ differs somewhat. The power law dependence of f describes $R_V/(R_V)_a$ at high functionality reasonable well (see Figure 7), but it emerges more slowly than for $R_G/(R_G)_a$. The following expressions are obtained by regression analysis for $f \geq 6$:

$$R_V/(R_V)_a = 1.36f^{0.304} \quad \text{(good solvents)} \qquad (13)$$

$$R_V/(R_V)_a = 1.29f^{0.279} \quad (\Theta \text{ conditions}) \qquad (14)$$

The results are practically the same for $f \geq 8$ or $f \geq 12$ but are different for $f \geq 4$.

The exponents are larger for $R_V/(R_V)_a$ than for $R_G/(R_G)_a$ (eq 11 and 12), and the order is reversed for good solvents and Θ solvents. This seems inconsistent with the fuzzy-sphere picture we suggested earlier, because that would require the exponents for $R_V(R_V)_a$ and $R_G/(R_G)_a$ to be the same. Thus, in the large f limit we expect

$$R_V/(R_V)_a = (1.29/1.17)[(R_G)_a/(R_V)_a](R_G/(R_G)_a) \qquad (15)$$

in which 1.29/1.17 is R_V/R_G for hard spheres, corrected for a deeper penetration of the hydrodynamic interaction, and $(R_G)_a/(R_V)_a$ is the value for linear chains ($(0.75)^{-1}$ in good solvents and $(0.83)^{-1}$ in Θ solvents from Table X). With these quantities, the power laws for $R_V/(R_V)_a$ can be predicted from eq 11 for good solvents and eq 12 for Θ solvents. The results are shown by the dashed lines in Figure 7. The prediction could be an asymptote for $R_V/(R_V)_a$ vs f at the Θ condition, but that seems not to be true for the data in good solvents. Either the oversimplified nature of the fuzzy-sphere analogy or the experimental scatter and sparcity of data at large f are at fault. We have been unable to decide on the basis of present evidence.

As a final point, it is interesting to consider the dependence of intrinsic viscosity on the branch point functionality at constant arm molecular weight. Thus, for the definition of R_V in eq 8

$$[\eta] = 6.32 \times 10^{24} R_V^3/M \qquad (16)$$

so the variation of $[\eta]$ with increasing f depends on the competition between an increasing R_V and an increasing $M = fM_a$. The span molecular weight for a star is $2M_a$, and the intrinsic viscosity of a linear polymer with that molecular weight is $[\eta]_{span} = 2^{\alpha}[\eta]_a$, where $[\eta]_a$ is the intrinsic viscosity of the unattached arm and α is the exponent in eq 5. Thus

$$[\eta]/[\eta]_{span} = [R_V/(R_V)_a]^3/2^{\alpha}f \qquad (17a)$$

or more simply[32]

$$[\eta]/[\eta]_{span} = (f/2)^{\alpha}g' \qquad (17b)$$

where g' is the intrinsic viscosity ratio (see below). If desired, $R_V/(R_V)_{span}$ and $R_G/(R_G)_{span}$ can also be obtained from the results in Table XI by dividing the corresponding values for $f \geq 3$ by those for $f = 2$.

Figure 10 shows $[\eta]/[\eta]_{span}$ vs f in good and Θ solvents, calculated with the values of $R_V/(R_V)_a$ in Table XI and α for linear chains in Table V. Starting from the defined

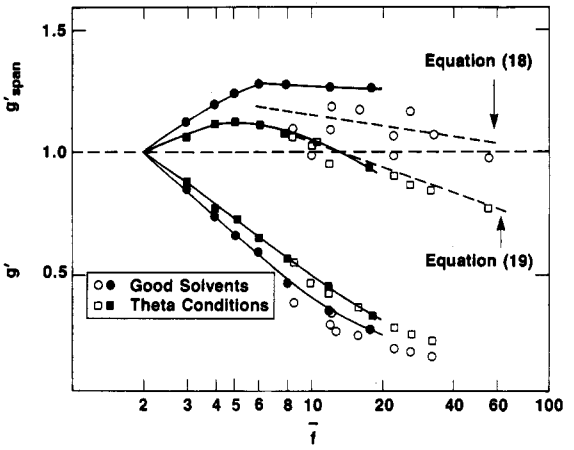

Figure 10. Values of g'_{span} and g' as a function of arm number for chlorosilane-linked (solid symbols) and divinylbenzene-linked (open symbols) polyisoprene stars. The Θ condition three-arm data point is for polystyrene.

value of unity at $f = 2$, $[\eta]/[\eta]_{span}$ increases at first, passes through a broad maximum, and finally decreases slowly as f becomes large. From eq 17a, the power law expressions at large f (eq 13 and 14) lead to

$$[\eta]/[\eta]_{span} = 1.51f^{-0.088} \quad \text{(good solvents)} \tag{18}$$

$$[\eta]/[\eta]_{span} = 1.52f^{-0.163} \quad (\Theta \text{ conditions}) \tag{19}$$

These results are shown as dashed lines in Figure 10. The addition of more branches in polymeric stars can apparently result in a lower intrinsic viscosity if f is already sufficiently large. In Θ solvents the intrinsic viscosity decreases with increasing f to values below those for the linear span ($f = 2$). In good solvents, it appears that $[\eta]$ may merely approach $[\eta]_{span}$ for large f.

Comparison with Theory

The experimental results for stars in dilute solution were presented and compared in the previous section in terms of equivalent molecular radii. Alternative schemes are available in which the radius of gyration, intrinsic viscosity, and molecular friction coefficient are compared with corresponding values for linear chains of the same total molecular weight:

$$g = R_G^2/(R_G^2)_L \tag{20}$$

$$g' = [\eta]/[\eta]_L \tag{21}$$

$$h = (D_0)_L/D_0 \tag{22}$$

Second virial coefficient–chain dimension relationships are expressed in terms of the penetration function[19]

$$\psi = A_2M^2/4\pi^{3/2}N_{av}R_G^3 \tag{23}$$

in which N_{av} is Avogadro's number. Intrinsic viscosity–chain dimension relationships are expressed in terms of the Flory coefficient[19]

$$\phi = [\eta]M/R_G^3 \tag{24}$$

Intrinsic viscosity–second virial coefficient relationships can be expressed in terms of[31]

$$\sigma = A_2M/[\eta] \tag{25}$$

In the dilute solution theories for f-arm star polymers, these quantities depend on f and differ for good solvents and Θ conditions, but, like the various radius ratios discussed earlier, they become independent of molecular weight for sufficiently long arms. The results of some theories have been expressed in terms of radius ratios and others in terms of the parameters defined by eq 20–24. It is therefore expedient to develop "translation" formulas based on the definitions of size used in eq 8–10 and the molecular weight exponents for linear chains as defined in eq 5–7:

$$R_G/(R_G)_a = g^{1/2}f^{\beta} \tag{26}$$

$$R_V/(R_V)_a = (g')^{1/3}f^{(1+\alpha)/3} \tag{27}$$

$$R_T/R_G = 1.10\psi^{1/3} \tag{28}$$

$$R_V/R_G = 5.41 \times 10^{-9}\phi^{1/3} \tag{29}$$

$$R_T/R_V = 0.856\sigma^{1/3} \tag{30}$$

$$R_V/R_H = (R_V/R_H)_L(g')^{1/3}h^{-1} \tag{31}$$

For regular stars with unperturbed (random walk) arm dimensions,[33] i.e., at the Θ condition and ignoring crowding effects in the core region

$$g_{rw} = (3f - 2)/f^2 \tag{32}$$

Diffusion coefficient and intrinsic viscosity have also been calculated analytically for random walk stars by using the Oseen approximation for hydrodynamic interactions and a preaveraging approximation for the intersegmental distances:[34,35]

$$h_{rw} = f^{1/2}/[(2 - 2^{1/2}) + (2^{1/2} - 1)f] \tag{33}$$

$$g'_{rw} \simeq g_{rw}^{1/2} \tag{34}$$

The latter is the Zimm–Kilb conjecture,[35] based on calculated values of $[\eta]$ for a limited range of functionalities. The Stockmayer–Fixman conjecture[34] is

$$g'_{rw} \simeq h_{rw}^3 \tag{35}$$

Monte Carlo methods have been used recently to circumvent preaveraging and to incorporate excluded volume effects. Values of g, g', and h for stars with 6, 12, and 18 arms were obtained in this way by Rey, Friere, and de la Torre.[36] Renormalization group methods have been applied to stars by Miyake, Douglas, and Freed[37,38] to obtain the leading terms of a series expression for g and ψ in good solvents. Daoud and Cotton used scaling arguments to allow explicitly for segmental crowding near the core of a multiarm star.[39] For long arms and large f they predict

$$R_G/(R_G)_a \simeq f^{1/5} \quad \text{(good solvents)} \tag{36}$$

$$R_G/(R_G)_a \simeq f^{1/4} \quad (\Theta \text{ condition}) \tag{37}$$

Grest, Kremer, and Witten have used a molecular dynamics simulation to examine the structure factor and chain dimensions for self-avoiding star polymers with up to 50 arms.[40]

The experimental values of $R_G/(R_G)_a$, $R_V/(R_V)_a$, and R_V/R_H at $f = 6$, 12, and 18 are compared in Table XII with values calculated from the Monte Carlo results[36] through eq 26, 27, and 31, respectively. The agreement for good solvents is excellent. The only significant departures are those for $R_G/(R_G)_a$ at the Θ condition, where the predicted values are consistently smaller than observed. We have also compared the data with other Monte Carlo results.[41–48] With one exception,[45] these have dealt with relatively low functionalities ($f \leq 6$) and are in reasonable agreement with the data on chain dimensions and dynamic behavior in that range. Barrett and Termain examined[45] chain dimensions for good solvents up to $f = 24$ and fit their results with the formula $g = 1.86f^{-4/5}$. With eq 26, this translates to $R_G/(R_G)_a = 1.36f^{0.178}$, in remarkably good agreement with our data (eq 11).

Table XII
Comparison of Experimental Results with Predictions Based on Monte Carlo Techniques[36]

	R_V/R_H		$R_G/(R_G)_a$		$R_V/(R_V)_a$	
f	theory	exptl	theory	exptl	theory	exptl
			Good Solvents			
1	1.11	1.11	1.0	1.0	1.0	1.0
6	1.04	(1.08)[a]	1.88	(1.82)[a]	2.35	2.30
12	1.02	(1.06)[a]	2.04	2.09	3.02	2.93
18	0.98	(1.06)[a]	2.19	2.23	3.20	3.36
			Θ Conditions			
1			1.0	1.0	1.0	1.0
6			1.72	1.88	2.05	2.13
12			1.99	2.10	2.53	2.60
18			1.95	2.30	2.78	2.85

[a] Values based on only a few samples or interpolated from the values of other functionalities.

Table XIII
Comparison of Experimental Results in Good Solvents with Predictions Based on Renormalization Group Techniques[37,38]

	$R_G/(R_G)_a$[37]		R_T/R_G[38]	
f	theory	exptl	theory	exptl
1	1.0	1.0	0.71	0.69
4	1.76	1.78	0.89	(0.83)[a]
6			1.04	(0.91)[a]
8	2.06	1.93	1.20	1.01
10			1.35	(1.06)[a]
16	2.49	(2.2)[a]		
32	3.14	(2.6)[a]		

[a] Values based on only a few samples or interpolated from the values for other functionalities.

Table XIV
Comparison of Experimental Results in Good Solvents with Molecular Dynamics Simulations[40]

	$R_G/(R_G)_a$			$R_G/(R_G)_a$	
f	simulation	exptl	f	simulation	exptl
1	1.0	1.0	30	2.51	2.60
6	1.93	1.82	40	2.64	2.70
10	2.09	2.01	50	2.76	2.80
20	2.31	2.30			

Comparisons of $R_G/(R_G)_a$ and R_T/R_G in good solvents with the renormalization group calculations[37,38] of g and ψ (through eq 26 and 28, respectively) are shown in Table XIII. Agreement is good when f is small, but the predicted values in both cases become consistently larger than observed as f increases. Calculations of ψ were not carried out for sufficiently large f to test whether the predicted values of R_T/R_G would level off near the hard-sphere value (see Figure 4).

Results of the molecular dynamics calculations for $R_G/(R_G)_a$ in good solvents[40] are compared with experiment in Table XIV. Agreement is excellent over the entire range ($1 \leq f \leq 50$). Both the molecular dynamics results and the experimental data are in reasonable accord with the scaling result for good solvents:[39] the predicted exponent is 0.20 (eq 36) and the observed exponent is 0.175 (eq 11). The observed exponent is slightly larger at the Θ condition (eq 12), as is the scaling prediction (eq 37). An explanation for the rapid approach to the asymptotic form has been suggested recently.[49]

We conclude with some comments about the analytical expressions based on random walk stars and the preaveraging approximation (eq 32–35) at the Θ condition. Thus, with eq 26, eq 32 leads to

$$R_G/(R_G)_a = (3 - 2/f)^{1/2} \quad (38)$$

while with eq 27, eq 32 and the Zimm–Kilb conjecture (eq 34) lead to

$$R_V/(R_V)_a = (3f^2 - 2f)^{1/6} \quad (39)$$

Likewise, eq 33 and the Stockmayer–Fixman conjecture (eq 35) lead to

$$R_V/(R_V)_a = f/[2 - 2^{1/2} + (2^{1/2} - 1)f] \quad (40)$$

Equations 38 and 40 systematically underestimate the values of $R_G/(R_G)_a$ and $R_V/(R_V)_a$ at the Θ condition, and, in fact, they predict that these quantities rather quickly approach limiting values with increasing f, contrary to the observations. Equation 39, on the other hand, provides a rather good discription of $R_V/(R_V)_a$ at the Θ condition up to $f \sim 8$. Beyond that range, the predicted values are too large by amounts that increase systematically with f, but even at $f = 50$ the error is only about 10%.

Summary and Conclusions

The radius of gyration, thermodynamic radius, viscometric radius, hydrodynamic radius, and Huggins coefficient were obtained in good solvents and at the Θ condition for nearly monodisperse polyisoprene stars with from 3 to 56 branches per molecule. When the arms are long, the ratios of radii are independent of arm molecular weight and vary systematically with the number of arms. For large arm numbers, these ratios settle into values near those for hard spheres. However, the equivalent radii derived from hydrodynamic properties are consistently smaller than those from equilibrium properties, suggesting an analogy between polymeric stars with many arms and spheres with a hydrodynamically penetrable surface layer. The same fuzzy-sphere picture seems to apply for both good solvents and Θ solvents and to polystyrene stars as well as those of polyisoprene stars. Some apparent inconsistencies with this simple interpretation were noted and could not be resolved on the basis of the available data.

The results were compared with theoretical predictions based on scaling arguments, analytical calculations, Monte Carlo methods, and simulations. Behavior of the radius of gyration agrees very well with the scaling predictions of Daoud and Cotton,[39] the molecular dynamics simulations of Grest, Kremer, and Witten,[40] and the Monte Carlo simulations of Rey, Freire, and de la Torre.[36] Viscometric and hydrodynamic radii are also reasonably consistent with the Monte Carlo results. Analytical predictions, whether derived from random walk models with preaveraging or from renormalization group calculations, are less satisfactory and are especially so at high functionalities. Crowding in the core region, growing progressively with arm number, seems a likely cause of those discrepancies.

In conclusion, we wish to mention the recent work of Roovers, Toporowski, and Martin,[50] which deals with polybutadiene stars with functionalities of 263–278, with the linking agent in these cases being a hydrosilated 1,2-polybutadiene. The extrapolation of our relations, eq 11–14, 18, and 19, to these functionalities yields values in excellent agreement with those of Roovers and co-workers.[50] The only exception to this is the good solvent ratio, $R_G/(R_G)_a$, where eq 10 yields a value of 3.7 while experiment yields 5.1 (excluding the star with the lowest arm molecular weight). It is possible that this discrepancy is related to the small arm molecular weights used in Roover's work, ranging from $M_a = 4.5 \times 10^3$ to 4.2×10^4. The crowding effects would be expected to be quite pronounced in good solvents for such highly branches stars with relatively short arms. Overall, the good agreement between our findings and those of Roovers, Toporowski, and

Martin[50] is indeed striking and gratifying.

Acknowledgment. The work at the University of Akron was supported in part by Grant DMR-79-08200 and Grant GH-32583X from the Polymers Program of the National Science Foundation and by a NATO fellowship (G.Q.) during 1976–77, provided by the Deutsche Akademischer Austauschdienst.

Appendix

Analysis of the dilute solution properties of polyisoprene stars requires at several places the corresponding data for linear materials. Results in the literature[2,6,7,16,51] for both good solvents and Θ conditions were used to develop the correlations for linear polyisoprene, summarized in Table V.

For good solvents, the cyclohexane and toluene data in ref 2, 6, 7, and 51 were used. The combination of intrinsic viscosity in both solvents gives eq 3 of the text; the correlations for those solvents individually are given in Table V. The R_G–M relationship for linear polyisoprene in cyclohexane (Table V) was determined from the combined results of ref 2 and 51. All samples in both studies were prepared at Akron, and we excluded the result for samples L-11 and L-16 in ref 51 because of uncertainties in their molecular weight distributions.

For the Θ condition, the data in ref 6, 7, and 16 were used. Slight deviations from true Θ were eliminated by the Burchard–Stockmayer–Fixman[52,53] procedure for intrinsic viscosity and the Baumann procedure[54] for R_G. The correlations were established in all cases by unweighted linear regression analysis. Light-scattering intensity data were interpreted as described in Appendix A of ref 55.

Registry No. Polyisoprene, 9003-31-0.

References and Notes

(1) (a) University of Akron. Present address: Polymers Division, National Institute of Standards and Technology, Gaithersburg, MD 20899. (b) Exxon Research and Engineering Co. (c) Exxon Research and Engineering Co. Present address: Princeton University, Department of Chemical Engineering, Princeton, NJ 08544. (d) Visiting scientist at University of Akron and Exxon Research and Engineering Co. Present address: University of Athens, Division of Chemistry, Athens (10680), Greece. (e) University of Akron. Present address: Metallgesellschaft AG, Reuterweg 14, Frankfurt a. M. Federal Republic of Germany.
(2) Davidson, N. S.; Fetters, L. J.; Funk, W. G.; Hadjichristidis, N.; Graessley, W. W. *Macromolecules* **1987**, *20*, 2614.
(3) Hadjichristidis, N.; Guyot, A.; Fetters, L. J. *Macromolecules* **1978**, *11*, 668.
(4) Hadjichristidis, N.; Fetters, L. J. *Macromolecules* **1980**, *13*, 191.
(5) Quack, G.; Hadjichristidis, N.; Fetters, L. J.; Young, R. N. *Ind. Eng. Chem. Prod. Res. Dev.* **1980**, *19*, 587.
(6) Tsunashima, Y.; Hirata, M.; Nemoto, N.; Kurata, M. *Macromolecules* **1988**, *21*, 1107.
(7) Hadjichristidis, N.; Roovers, J. E. L. *J. Polym. Sci., Polym. Phys. Ed.* **1974**, *12*, 2521.
(8) Bauer, B. J.; Hadjichristidis, N.; Fetters, L. J.; Roovers, J. *J. Am. Chem. Soc.* **1980**, *102*, 2410.
(9) Roovers, J. E. L.; Bywater, S. *Macromolecules* **1972**, *5*, 385.
(10) Roovers, J. E. L.; Bywater, S. *Macromolecules* **1974**, *7*, 443.
(11) Zilliox, J.-G. *Makromol. Chem.* **1972**, *156*, 121.
(12) Huber, K.; Burchard, W.; Fetters, L. J. *Macromolecules* **1983**, *16*, 2287.
(13) Khasat, N.; Pennisi, R. W.; Hadjichristidis, N.; Fetters, L. J. *Macromolecules* **1988**, *21*, 1100.
(14) Candau, F.; Rempp, P.; Benoit, H. *Macromolecules* **1972**, *5*, 627.
(15) Richter, D.; Stühn, B.; Ewen, B.; Nerger, D. *Phys. Rev. Lett.* **1987**, *58*, 2462.
(16) Hadjichristidis, N.; Xu, Z.; Fetters, L. J.; Roovers, J. *J. Polym. Sci., Polym. Phys. Ed.* **1982**, *20*, 743.
(17) Roovers, J.; Toporowski, P. M. *J. Polym. Sci., Polym. Phys. Ed.* **1980**, *18*, 1907.
(18) Akcasu, A. Z.; Benmouna, M. *Macromolecules* **1978**, *11*, 1193.
(19) Yamakawa, H. *Modern Theory of Polymer Solutions*; Harper and Row: New York, 1971.
(20) Batchelor, G. K. *J. Fluid Mech.* **1977**, *83*, 97.
(21) The k_H values for the four- and six-arm stars are from the samples studied in ref 7. These values have heretofore been unpublished.
(22) Peterson, J. M.; Fixman, M. *J. Chem. Phys.* **1963**, *39*, 2516.
(23) Freed, K. F.; Edwards, S. F. *J. Chem. Phys.* **1975**, *62*, 4032.
(24) Imai, S. *Proc. R. Soc. London, A* **1969**, *308*, 497.
(25) Ogasa, T.; Imai, S. *J. Chem. Phys.* **1971**, *54*, 2989.
(26) Muthukumar, M. *J. Chem. Phys.* **1983**, *79*, 4048.
(27) Xu, Z.; Qian, R.; Hadjichristidis, N.; Fetters, L. J. *J. China Univ. Sci. Technol.* **1984**, *14*, 228.
(28) Masuda, T.; Ohta, Y.; Yamauchi, T.; Onogi, S. *Polym. J. (Tokyo)* **1984**, *16*, 273.
(29) Mays, J. W.; Hadjichristidis, N.; Fetters, L. J. *Polymer* **1988**, *29*, 680.
(30) (a) Mays J. W.; Hadjichristidis, N.; Fetters, L. J. *Macromolecules* **1985**, *18*, 2231. The results of this reference when coupled with those of ref 29 show that the Θ condition $R_V/(R_V)_a$ ratios for polystyrene stars are independent of temperature over the range from 10 to 70 °C. (b) See, for example: Kunz, D.; Thurn, A.; Burchard, W. *Polym. Coll. Sci.* **1983**, *261*, 635. These authors found that R_H/R_G was larger than the hard-sphere value for microgel particles but smaller for casein aggregates.
(31) Davidson, N. S.; Fetters, L. J.; Funk, W. G.; Graessley, W. W.; Hadjichristidis, N. *Macromolecules* **1988**, *21*, 112.
(32) Bauer, B. J.; Fetters, L. J. *Rubber Chem. Technol.* **1978**, *51*, 406.
(33) Zimm, B. H.; Stockmayer, W. H. *J. Chem. Phys.* **1949**, *17*, 1301.
(34) Stockmayer, W. H.; Fixman, M. *Ann. N.Y. Acad. Sci.* **1953**, *57*, 334.
(35) Zimm, B. H.; Kilb, R. W. *J. Polym. Sci., Part B* **1959**, *37*, 19.
(36) Rey, A.; Freire, J. J.; de la Torre, J. G. *Macromolecules* **1987**, *20*, 342.
(37) Miyake, A.; Freed, K. F. *Macromolecules* **1983**, *16*, 1228.
(38) Douglas, J. F.; Freed, K. F. *Macromolecules* **1984**, *17*, 1854.
(39) Daoud, M.; Cotton, J. P. *J. Phys. Chem.* **1982**, *43*, 531.
(40) Grest, M.; Kremer, K.; Witten, T. *Macromolecules* **1987**, *20*, 1376.
(41) Zimm, B. H. *Macromolecules* **1984**, *17*, 795.
(42) Zimm, B. H. *Macromolecules* **1984**, *17*, 2441.
(43) Whittington, S. G.; Lipson, J. E. G.; Wilkinson, M. K.; Gaunt, D. S. *Macromolecules* **1986**, *19*, 1241.
(44) Wilkinson, M. K.; Gaunt, D. S.; Lipson, J. E. G.; Whittington, S. G. *Macromolecules* **1988**, *21*, 1818.
(45) Barrett, A. J. Termain, D. L. *Macromolecules* **1987**, *20*, 1687.
(46) Croxton, C. A. *Polym. Commun.* **1988**, *29*, 2.
(47) Croxton, C. A. *Macromolecules* **1988**, *21*, 2269.
(48) Ross-Murphy, S. B. *Polymer* **1978**, *19*, 497. The Monte Carlo approach used in this paper leads to low values, relative to experimental results, for stars under Θ conditions for $\bar{f}$ up to 10.
(49) Batoulis, J.; Kremer, K., submitted for publication in *Macromolecules*.
(50) Roovers, J.; Toporowski, P.; Martin, J. *Macromolecules*, in press.
(51) Tsunashima, Y.; Hirata, M.; Nemoto, N.; Kurata, M. *Macromolecules* **1987**, *20*, 1992.
(52) Burchard, W. *Makromol. Chem.* **1960**, *50*, 20.
(53) Stockmayer, W. H.; Fixman, M. *J. Polym. Sci., Part C* **1963**, *1*, 137.
(54) Baumann, H. *J. Polym. Sci., Part B* **1965**, *3*, 1069.
(55) Colby, R. N.; Graessley, W. W.; Fetters, L. J. *Macromolecules* **1987**, *20*, 2226.